Proceedings of ERAD 2006

Drop shape probability contours in rain from 2-D video disdrometer: implications for the 'self consistency method' at C-band

M. Thurai[1], **G.J. Huang**[1] **V.N. Bringi**[1] **and M. Schönhuber**[2]
[1]Colorado State University, Fort Collins, CO 80523-1373, USA
[2]Joanneum Research, Graz, Austria

1 Introduction

The so-called self consistency method uses the fact that the true radar co-polar reflectivity (Z_h^{true}) and the differential reflectivity (Z_{dr}^{true}) can be used to predict the specific differential propagation phase (K_{dp}) at each radar range gate. The application of this method at S-band is relatively straight-forward as has been demonstrated in the past (e.g. Goddard et al., 1994). At C-band, one needs to correct for co-polar attenuation and differential attenuation for the measured Z_h and Z_{dr} respectively and this is done on a gate-to-gate basis (Tan et al, 1995) using the K_{dp} profile derived from the measured range profile of the differential propagation phase (Φ_{dp}). The corrected Z_h and Z_{dr} are used to estimate the K_{dp} at each range gate and hence also the range profile of the Φ_{dp}, which is then compared with the measured Φ_{dp} profile. The comparisons are sensitive to the Z_h calibration and hence this procedure ensures that the external radar calibration is accurate. The method is also capable of correcting for rain-on-radome effects in near-real time (Thurai and Hanado, 2005, Bringi et al. 2006). The accurately calibrated and corrected Z_h and Z_{dr} range profiles for each radar scan ensures that the subsequent estimates of drop size distributions and rainfall rates derived from the polarization data are also accurate.

However, the self-consistency method requires pre-defined relationships to be formulated between the specific attenuation (A_H) and K_{dp} as well as the specific differential attenuation (A_{dp}) and K_{dp}. In addition, for the final self consistency checks to be performed, the relationship between the ratio K_{dp} / Z_h^{linear} and Z_{dr} is also required.

Correspondence to: Merhala Thurai
merhala@engr.colostate.edu

In the earlier study (Thurai and Hanado 2005) using the C-band polarimetric radar data, drop axis ratios and drop size distributions (*DSD*) derived from a 2-dimensional disdrometer (2DVD; see Randeu et al. 2002) located 15 km from the radar site were used to derive these relationships. For convenience, the drop shapes were approximated to their equivalent oblate spheroids (with axis ratios given by the maximum vertical to the maximum horizontal chords) to derive the necessary relationships.

In this paper, we report on the actual probability contours of drop shapes obtained directly from the fast scanning cameras of the 2DVD. Using these more accurately contoured shapes as well as the measured *DSD*s, we examine if the abovementioned relationships need to be modified at C-band. Contour comparisons are also made with the Beard and Chuang (1987) equilibrium shape (static) numerical model for different diameters.

2 Previous analysis assuming oblate spheroids

Data from the C-band radar (belonging to the National Institute of Information and Communications Technology, NICT, of Japan) and the 2DVD used in the previous study were taken in Okinawa, Japan, during the Baiu season in 2004. Bringi et al. (2006) have provided detailed analysis of this event, which included the radar and the 2DVD as well as a 400 MHz wind profiler. In the process of comparative analysis, it was found that the self-consistency method could be applied to determine the external radar calibration factor, including correction due to rain-on-radome which depended on the rain intensity at and near the radar site. The relationships used in the self consistency method were of the form:

$$A_H = a_1 K_{dp}; dB/km \quad (1a)$$

$$A_{dp} = a_2 K_{dp}^{a_3}; dB/km \quad (1b)$$

$$\frac{K_{dp}}{Z_h^{linear}} = a_4 \left(Z_{dr}^{a_5} \right); deg/km\ per\ mm^6\ m^{-3} \quad (2)$$

where the coefficients a_1 to a_5 were obtained from the analysis of the simultaneous measurements from the 2DVD. 1 minute integrated *DSD*s were used, together with the approximated spheroid shapes, both being derived from the 2DVD data. T-matrix calculations were performed to obtain the parameters Z_H, Z_{dr}, K_{dp}, A_H and A_{dp} corresponding to each of the 1-minute *DSD*s. From these, the coefficients a_1 to a_5 were determined by best power-law fits between the relevant parameters.

3 Drop shapes from the Okinawa event

The images captured during this event by the 2DVD's fast scanning cameras were reprocessed using a contour smoothing procedure to construct the actual shape of each individual drop. Full details of the contour smoothing algorithms for the 2DVD data as well as their implementation can be found in Gimpl (2003), but a brief summary is given in the Appendix. Each drop, after undergoing contour smoothing, was categorized into various equi-volumetric sphere diameter intervals, ranging from 1.5 to 8 mm in 0.25 mm steps. Below 1.5 mm, the resolution of the 2DVD was not considered sufficient for accurate shape estimation. For each of the assigned diameter intervals, all drop contours in that category were superimposed exactly on each other to derive the probability contours, the probability values being normalized to the total number of pixels in all the drop contours in that diameter interval. Figure 1 shows greyscale images of these probability contours (in log scale) for equivalent drop diameters in the range (a) 3 – 3.25 mm, (b) 4 - 4.25 mm. Superimposed on the plots in white are the Beard-Chuang (1987) (B-C) equilibrium shapes, derived from the summation of cosine series, the coefficients of which are given in Table 4 of their article. The agreement is close.

4 Larger drops

The Baiu event lasted over several hours; however it produced very few drops larger than 5 mm and hence it is not possible to compare the B-C model for large drops for this event. However, an earlier experiment (Thurai and Bringi 2006) consisting of artificial rain with drops falling over 80 m, did produce considerable number of large drops and their contour analysis showed that the larger drops tended to have flatter bases (Thurai et al 2006). Two examples are shown in Figure 2 for (a) 5-5.25 mm and (b) 6-6.25 mm. The flat bases are evident, particularly for the larger diameter. The superimposed B-C curves, once again show good agreement, although slight deviation becomes evident at the base of the 6-6.25 mm drops when viewed on an enlarged scale.

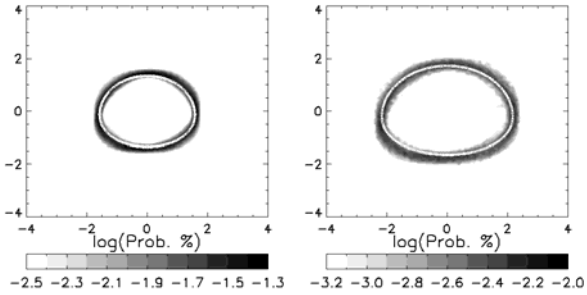

Fig. 1: Drop shapes given in terms of probability contours on a log scale indicated in grey scale for 3-3.25 mm (left), 4-4.25 mm (right) from the Okinawa event compared with the Beard-Chuang curves in white.

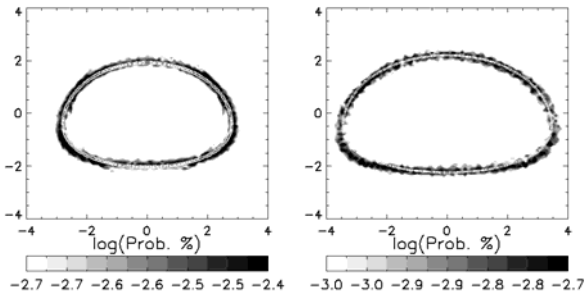

Fig. 2: Drop shapes for 5-5.25 mm (left), 6-6.25 mm (right) from the 80 m fall experiment, again compared with the Beard-Chuang curves.

5 Fitted equation

For the purpose of calculating the radar parameters, the mean contour drop shapes were fitted to a mathematical representation of smoothed conical-like shapes, given in Wang (1982), given by:

$$x = c_1 \sqrt{1 - \left(\frac{y}{c_2}\right)^2} \left[\cos^{-1}\left(\frac{y}{c_3 c_2}\right) \right] \left[c_4 \left(\frac{y}{c_2}\right)^2 + 1 \right] \quad (3)$$

where x and y are the cartesian coordinates and the parameters c_1, c_2, c_3 and c_4 were fitted to obtain the mean dependence on the equi-volumetric sphere diameter (D_{eq} in mm), given by:

$$c_1 = \frac{1}{\pi}\left(0.02914 D_{eq}^2 + 0.9263 D_{eq} + 0.07791\right)$$

$$c_2 = -0.01938 D_{eq}^2 + 0.4698 D_{eq} + 0.09538$$

$$c_3 = -0.06123 D_{eq}^3 + 1.3880 D_{eq}^2 - 10.41 D_{eq} + 28.34$$

$$c_4 = -0.01352 D_{eq}^3 + 0.2014 D_{eq}^2 - 0.8964 D_{eq} + 1.226 \quad for\ D_{eq} > 4\,mm$$

$$c_4 = 0 \quad for\ D_{eq} \le 4\,mm$$

c_1, c_2 and c_3 are the same parameters a, c and λ as in Wang (1982).

6 T-matrix calculations

Calculations using the T-matrix method were performed for the 1 minute integrated *DSD*s measured by the 2DVD during the long Baiu event in Okinawa. The contoured shapes given by the fitted equation (3) were used for the calculations and compared those assuming approximated oblate spheroids given by:

$$\frac{b}{a} = 1.065 - 6.25\times10^{-2}\left(D_{eq}\right) - 3.99\times10^{-3}\left(D_{eq}^2\right) + 7.66\times10^{-4}\left(D_{eq}^3\right) - 4.095\times10^{-5}\left(D_{eq}^4\right) \quad for\ D_{eq} > 1.5\,mm \quad (4a)$$

$$\frac{b}{a} = 1.17 - 0.516\left(D_{eq}\right) + 0.47\left(D_{eq}^2\right) - 0.132\left(D_{eq}^3\right) - 8.5\times10^{-3}\left(D_{eq}^4\right) \quad for\ 0.7 \le D_{eq} \le 1.5\,mm \quad (4b)$$

$$\frac{b}{a} = 1 \quad for\ D_{eq} < 0.7\,mm \quad (4c)$$

(4a) is a re-fitted formula to the drop axis ratios given in Thurai and Bringi (2005), (4b) is a fitted formula to the axis ratios for small drops given in Beard and Kubesh (1991) and (4c) assumes spherical drops for D_{eq} < 0.7 mm.

Fig. 3 shows the comparisons for the radar parameters Z_{dr} and K_{dp} at 5.34 GHz. Over 1600 1-minute *DSD*s are represented in the figure. Their fitted linear equations are also shown in the plots. They show very good agreement between the contoured shapes and their approximated versions of oblate spheroids. Although they represent rainfall rates ranging up to 100 mm/h, over 80% of the cases had rain rates less than 10 mm/h. Hence, the best-fitted regression lines are weighted towards the stratiform, less intense periods of the event (Bringi et al. 2006). Nevertheless, as seen in Fig. 4, the fitted lines also give good agreement for the higher values for both cases of computed parameters.

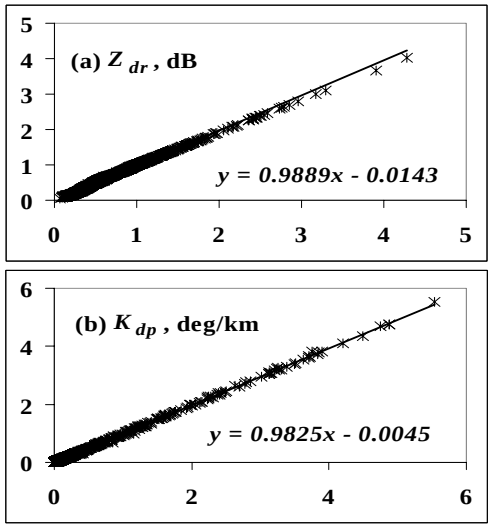

Fig. 3: Comparisons of (a) Z_{dr} and (b) K_{dp}, using the contoured shapes (x-axis) and the approximated oblate spheroids (y-axis). Equations for the best fitted lines are also given.

The comparisons for Z_H, Z_{dr}, K_{dp}, A_H and A_{dp} are given in terms of the linear regression parameters (y=ax+b) in Table 1. In all five cases, the regression lines are close to the line of equality, thus suggesting that any relationships derived between the five parameters will not be affected significantly by approximating the shapes to oblate spheroids. In other words, the coefficients a_1 to a_5 in (2a) to (2c) need not be altered to account for the non-oblate shapes. Note, the *DSD*s considered here did not have significant number of large drops (above 5 mm). Thurai et al (2006) have also considered unusual *DSD*s with large median volume diameter which show an underestimation of Z_{dr} by as much as 8% at C-band when the oblate-spheroid approximation is used for the T-matrix calculations. For such cases, one would need to derive the relationships equivalent to (1a), (1b) and (2) using the actual contoured shapes.

Table 1: Comparisons in terms of the regression line equations for the various parameters

Parameter	Equation of best-fit line
Z_H	$y = 1.01x - 0.13$
Z_{dr}	$y = 0.99x - 0.01$
K_{dp}	$y = 0.98x - 0.00$
A_H	$y = 1.04x - 0.00$
A_{dp}	$y = 1.00x - 0.00$

7 Conclusions

Drop shapes derived from the fast line scan cameras of the 2DVD have been presented. For equi-volumetric diameters up to 4 mm, the shapes seem to be close to oblate spheroids. Larger drops show more flattened base, in agreement with the Beard and Chuang shapes. T-matrix calculations of polarimetric radar parameters using over 1600 1-minute *DSD*s measured in a sub-tropical location during a prolonged event show that the oblate spheroid equivalent shapes could be used to a good approximation to derive the relationships necessary to implement the self-consistency method at C-band. However, unusual events with large median volume diameters would need to have their contoured shapes used for attenuation correction schemes.

Acknowledgements

This work was supported by the National Science Foundation via grant ATM-0603720. The 2DVD data from Okinawa were kindly provided by Dr. K. Nakagawa of NICT, Japan.

Appendix A: 2DVD Data Contour Smoothing

2DVD data describe raindrops' contours by shadowed grid points. Threshold discrimination judges the camera pixels' gray scale values as illuminated or shadowed, together with the grid resolution (finer than 0.2 mm) inducing a quantisation uncertainty range around the true shape of a contour. To provide an estimate for true contour points, first the inner and outer boundary of the uncertainty range are processed separately. Digital image processing standard literature explains a number of curve modelling techniques. The Akima Interpolation was evaluated as best suited: it results in a smooth line including all base points, it does not assume some functional form of the whole curve but the result depends on base points in immediate neighbourhood only, and it is computationally effective since it only needs to solve small equation systems. The outward pointing corners of the outer boundary and the inward pointing ones of the inner boundary are chosen as base points for smoothing by Akima Interpolation. After that, considering a point at the centroid, each radial ray cuts both, the inner and outer smoothed boundaries. On each ray, these two intersection points are used to give a weighted vectorial mean, with the weights differing only slightly from 50%, to ensure correct reproduction of calibration spheres. This 2DVD data contour smoothing method was confirmed as reliable and useful, qualitatively by visual assessment of results and quantitatively by confirmation that for each calibration sphere size the method on average does not give rise to changes bigger than 1 percent, neither in the contours' area, nor in their height-to-width ratio (Thurai et al. 2006).

References

Beard, K.V. and C. Chuang, 1987: A New Model for the Equilibrium Shape of Raindrops. *J. Atmos. Sci.*, **44**, 1509-1524.

Beard, K.V. and R.J. Kubesh 1991: Laboratory Measurements of Small Raindrop Distortion. Part 2: Oscillation Frequencies and Modes, *J. Atmos. Sci.*, **48**, 2245-2264.

Bringi, V. N., M. Thurai , K. Nakagawa , G.J. Huang, T. Kobayashi, A. Adachi, H. Hanado, and S. Sekizawa, 2006: Rainfall estimation from C-band polarimetric radar in Okinawa, Japan: Comparisons with 2D-video disdrometer and 400 MHz Wind Profiler, *J. Met Soc of Japan*, **84** (4), Aug. 2006 issue, *in print*.

Gimpl, J. 2003: Optimised Algorithms for 2D-Video-Distrometer Data Analysis and Interpretation, Diploma Thesis, Institute of Communications and Wave Propagation, Graz University of Technology, Austria, supervised by W.L. Randeu and M. Schönhuber, p. 111.

Goddard, J.W.F., J. Tan, and M. Thurai, 1994: A technique for the calibration of Meteorological Radars using Differential Phase, *Electronics Letters*, **30**, (2), 166-167

Randeu, W.L., M. Schönhuber and G. Lammer, 2002: Real-time Measurements and Analyses of Precipitation Micro-structure and Dynamics. *Proc. of ERAD(2002)*, 78-83.

Tan, J, J.W.F. Goddard, and M. Thurai, 1995: Applications of Differential Propagation Phase in Polarisation-Diversity Radars at S-Band and C-Band, *Proc. Int. Conf. on Antennas and Propagation*, Eindhoven, NL, 336-341.

Thurai, M. and V.N. Bringi, 2005: Drop Axis Ratios from 2D Video Disdrometer, *J Atmos. Ocean. Tech*, **22**, 963-975.

Thurai M. and H. Hanado 2005: 'Absolute calibration of C-band weather radars using differential propagation phase in rain', *Electronics Letters*, 2005, **41 (**25), 1405-1406.

M. Thurai, G.J. Huang, V.N. Bringi, W. L. Randeu, M. Schönhuber: 2006, Drop shapes, model comparisons and calculations of polarimetric radar parameters in rain, Submitted to *J. Atmos. Ocean. Tech.*

Wang, P.K.: Mathematical description of the shape of conical hydrometeors, *J. Atmos. Sci.*, 1982, **39**, 2615-2622.